RAPID COMMUNICATIONS

PHYSICAL REVIEW A VOLUME 51, NUMBER 1 JANUARY 1995

Ultracold photoassociative ionization collisions in an atomic beam: Optical field intensity and polarization dependence of the rate constant

C.-C. Tsao, R. Napolitano, Y. Wang, and J. Weiner

Department of Chemistry and Biochemistry, University of Maryland, College Park, Maryland 20742

(Received 10 March 1994)

We report here measurements of two-body photoassociative ionization collisions between sodium atoms within an ultranarrow velocity class selected from a well-collimated, thermal atomic beam. Doppler-shifted excitation of the $Na(3s\ ^2S_{1/2};F=1)\rightarrow Na(5p\ ^2P_{3/2})$ transition at 285 nm by a single-mode laser defines the narrow velocity class that subsequently populates the $F=2$ hyperfine level of the Na ground state by optical pumping. Probe laser beam excitation tuned near the $Na(3s\ ^2S_{1/2};F=2)\rightarrow Na(3p\ ^2P_{3/2};F=3)$ transition produced photoassociative ionization with an average collision energy E_K corresponding to a temperature of 5.3 mK ($E_K=\frac{3}{2}kT$). We determine the rate constant for the process as a function of probe beam intensity and polarization.

PACS number(s): 32.80.Pj, 33.80.Ps, 34.50.Rk, 34.80.Qb

The past five years have witnessed a heightened interest in the physics of atomic collisions in the "ultracold" regime where the duration of a two-body encounter becomes long compared to spontaneous radiative emission of the system. Ultracold excited-state collisions are truly novel because, at the extremely long time and distance scales inherent in this regime, dissipative coupling to the radiation field becomes significant and inelastic collision probabilities become subject to optical manipulation. Reports of optical atom cooling [1] inspired early calculations of photon-stimulated two-body association reactions [2], and the first experiments on associative ionization between optically cooled sodium atoms [3,9] demonstrated that the inelastic rate constant could be dramatically modified by intensity modulation of the radiation field. Recent one-color [4] and two-color [5] spectroscopy measurements of the collision intermediate have revealed the important role played by hyperfine structure in the collision mechanism. "Catalysis" lasers used to probe trap-loss collisions in a MOT (magneto-optical trap) [6] also show spectral features which underscore the molecular nature of the light absorption. Experiments in Rb [7] show a surprisingly pronounced (and as yet not entirely understood) isotope effect in the fine-structure-changing collision rate constant. All these trap experiments clearly illustrate the active role played by the frequency and intensity of optical fields in ultracold collisions. However, optical probing of the trapped and cooled atoms within about 200 MHz of the cycling transition appears to so greatly alter their internal states as to essentially destroy the trap. We report here an alternative approach to trap experiments in which we directly measure the intensity and polarization dependence of ultracold photoassociative ionization (PAI) collisions,

$$Na+Na+2h\nu\rightarrow Na_2^{+}+e, \tag{1}$$

taking place within a narrow velocity group selected from a collimated atomic beam and excited within 10 MHz of atomic resonance. Previous studies have demonstrated that one- or two-color light fields initiate PAI by a two-step process [5,8,9]. In the first step incoming ground-state reactant atom pairs absorb a photon to excited attractive states at very long range. Subsequent acceleration on the $-C_3/R^3$ attractive potential to shorter range together with absorption of a second photon (of the same or different color) to a doubly excited state leads to the final collision product. The beam technique separates the velocity-group selection field from the probe field, thus enabling independent variation of probe-field parameters without altering the characteristics of the initial atomic ensemble. The atomic beam geometry also maintains a well-defined collision reference axis on which probe-field polarization (linear or circular) can align or orient collision pairs. The present work builds on earlier collision studies [10] in which the Na $D2$ line provided the group-selecting transition. The natural width of the D line ($\simeq 10$ MHz), however, corresponds to a dispersion of intragroup velocities which sets the lower limit on collision energy to about 65 mK, just above the temperature T_S at which the time of collision becomes comparable to the radiative lifetime (64 mK for Na) [11]. In the present work we have devised a scheme in which the Na ($3s\leftrightarrow 5p$) line selects the velocity group. With a natural width of 0.65 MHz this transition leads to a selected velocity class with average collision energy well below the T_S threshold. Figure 1 shows a schematic of the experiment. Sodium vapor emerges from a hole in a heated oven and passes through a beam-defining collimation aperture. A single-mode ring dye laser (beam 1), locked to the $Na(3s\ ^2S_{1/2};F=2)\rightarrow Na(3p\ ^2P_{3/2};F=2)$ transition, crosses the atomic beam at right angles and pumps all the ground-state $F=2$ population to the $F=1$ level. An angle-tuned potassium dihydrogen phosphate (KDP) crystal, inserted into the ring of a second dye laser, produces about 5.7 mW cm^{-2} of second harmonic uv near 285 nm and tuned about 2.4 GHz to the red of the $3s\ ^2S_{1/2}\rightarrow 5p\ ^2P_{3/2}$ transition. The uv beam (beam 2) crosses the atomic beam at an angle of 5°, almost antiparallel to the atom flux. Beam 2 excites a narrow velocity group on the Doppler-shifted $3s\rightarrow 5p$ transition near the peak of the distribution of velocities in the atomic beam and pumps it to the previously emptied $F=2$ level of the ground state. The small crossing angle between beam 2 and the sodium beam maximizes the interaction zone and ensures efficient optical pumping, even at

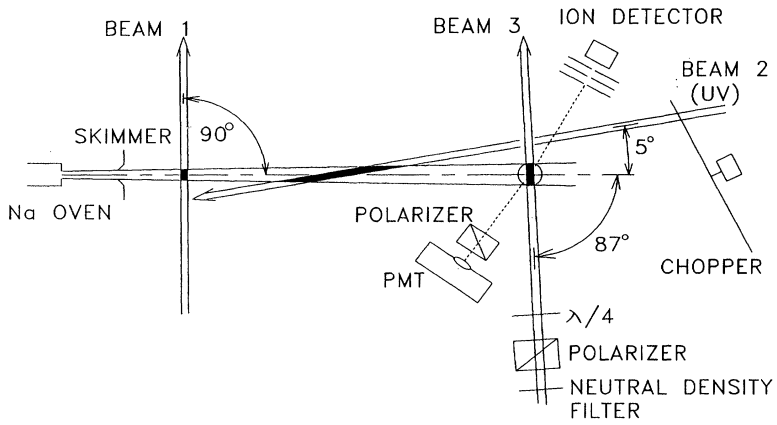

FIG. 1. Schematic diagram of the apparatus. Ion detector axis is perpendicular to the plane of the crossed beams.

low power density in beam 2. At a distance 180 mm downstream from the beam-2 excitation region, the selected velocity group encounters a probe laser beam (beam 3) tuned near the Na($3s\ ^2S_{1/2};F=2$)→Na($3p\ ^2P_{3/2};F=3$) transition and crossed at 87° to match the Doppler shift of the selected velocity group. A charged-particle multiplier mounted vertically above the plane formed by the crossed beams detects and amplifies the Na_2^+ ion pulses arising from photoassociative ionization collisions. Charged-particle imaging and aperturing insure that only ions formed in the beam-3 interaction zone are detected and that ion collection efficiency in this zone is near unity. We define the intensity-dependent rate constant $k(I)$ as

$$\frac{d[Na_2^+]}{dt}=k(I)[Na]^2, \tag{2}$$

where [Na] is the density of the selected velocity group. Measurements of the ion count rate, atomic beam density (via Beer's law absorption of a weak, resonant probe beam), and interaction volume determine the rate constant for the process. Overlap of beam 3 (0.6 cm diameter) with the narrower atomic beam (0.3 cm diameter) defines the interaction volume. The experiment measures the rate constant as a function of beam-3 intensity and polarization (parallel or perpendicular to the atomic beam axis). During an experimental run, beam 1 is locked to the center of the resonance line to ensure that optical pumping of the $F=2$ level remains uniform and efficient throughout the data-taking session. A mechanical wheel chops beam 2 at 130 Hz, modulating the ion signal, which is fed to a gated counter. As a check on the probe beam frequency stability, a separate photomultiplier tube monitors fluorescence of the velocity group excited by beam 3, while a calibrated power meter measures its intensity. The thoroughness of beam-1 optical pumping of the ground-state $F=2$ level is checked by blocking beam 2 (thereby preventing velocity-class repopulation of this level) and probing for residual population with beam 3. Both fluorescence and ion signals fall below detectable limits (2 counts/min). The maximum signal rate from the experiment is low (about 1 count/sec), but the average signal-to-noise ratio is about 8. Hyperfine structure of the $5p\ ^2P_{3/2}$ level leads to the formation of a "triplet" structure in the velocity group ($5p\ ^2P_{3/2};F=2,1,0$) with a spectral width of each component ≃1.4 MHz and an overall spectral width of about 8 MHz. The optical pumping efficiency of these subgroups is a function of the frequency, intensity, and polarization of beam 2, and therefore the net, effective velocity group spectrum must be calculated from the full set of 349 coupled optical Bloch equations (OBE's) describing the excitation from Na($3s\ ^2S_{1/2};F=1$) to the hyperfine levels of Na ($5p\ ^2P_{3/2}$) and subsequent relaxation (via spontaneous emis-

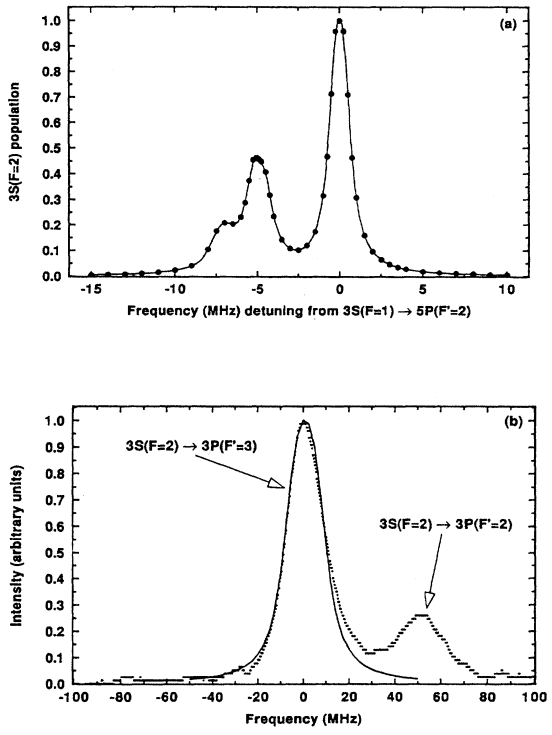

FIG. 2. (a) Velocity class distribution, calculated from coupled optical Bloch equations, and showing contributions from the hyperfine components of the $5p\ ^2P_{3/2}$ level. The peaks from right to left correspond to $F=2,1,0$. (b) Comparison of calculated velocity group profile (solid curve) under experimental conditions and directly measured profile (dotted curve).

sion) to Na($3s\ ^2S_{1/2};F=2$). We have carried out this calculation including all non-negligible off-diagonal state coherences and all relaxation terms [12] for the actual experimental conditions of beam-2 intensity, frequency, polarization, and atom flux residence time within beam 2. Figure 2(a) shows the resulting frequency spectrum of the Na($3s\ ^2S_{1/2};F=2$) ground-state population. This spectrum maps to velocity space v through the simple Doppler-shift expression,

$$\Delta\nu=\nu-\nu_0=\frac{v\cos\theta}{\lambda_0}, \tag{3}$$

where ν_0,λ_0 are the rest frequency and wavelength of the Na($3s\leftrightarrow 5p$) transition, and θ is the angle between beam 2 and the atomic beam. The OBE calculations were checked against direct measurements of the velocity-group profile by folding in the additional experimental conditions of atomic beam divergence and beam-3 spectral width and power broadening. Figure 2(b) compares the simulated and directly measured profiles which show excellent agreement. The distribution of axial relative collision velocities in the selected group $P(V_A)$ is given by the autocorrelation of the group distribution calculated from the OBE's,

$$P(V_A)=\int_0^{+\infty}dv_2\int_0^{+\infty}dv_1 p(v_1)p(v_2)\delta(|v_1-v_2|-V_A), \tag{4}$$

where $p(v_1),p(v_2)$ are the axial velocity distributions of atoms 1,2 and $|v_1-v_2|$ is the absolute value of the relative collision velocity. The average axial collision velocity $\langle V_A\rangle$ and energy $\langle E_A\rangle$ are then given by

$$\langle V_A\rangle=\int_0^{\infty}V_A P(V_A)dV_A \tag{5}$$

and

$$\langle E_A\rangle=\frac{\mu}{2}\langle V_A^2\rangle=\frac{\mu}{2}\int_0^{\infty}V_A^2 P(V_A)dV_A\,. \tag{6}$$

Transverse velocity components V_T from the atomic beam divergence (1.8 mrad) also contribute to the total average collision velocity $\langle V_C^2\rangle=[(\langle V_A^2\rangle+2\langle V_T^2\rangle)]$. In the present setup $\langle V_T\rangle=1.6$ m sec^{-1}. With

$$\tfrac{1}{2}\mu\langle V_C^2\rangle=\tfrac{3}{2}kT \tag{7}$$

we find $T=5.3$ mK. Beam 3 is also used to carry out a Beer's law measurement of the atomic beam ground-state density n (at the PAI interaction zone) by measuring resonant absorption and applying $\ln(I/I_0)=-n\sigma F(\omega)x_0$, where σ, $F(\omega)$, x_0 are the absorption cross section, line-shape factor, and atomic beam width, respectively. Using this expression we calculate an atomic beam density $\simeq 10^8$ cm^{-3} from which we obtain the velocity group density. The velocity group density, in turn, is inserted into (2) to calculate the

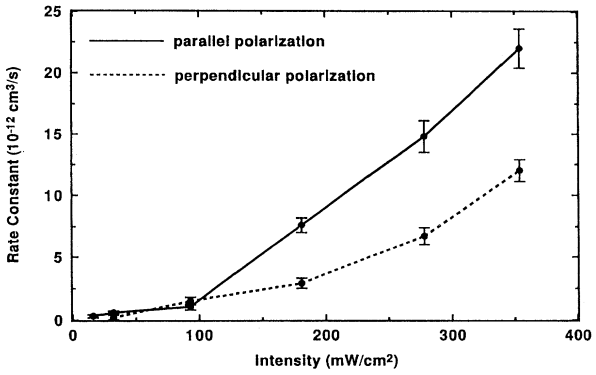

FIG. 3. Rate constant of PAI vs intensity of beam 3 for polarization parallel and perpendicular to atomic beam axis. Error bars show uncertainty due to random, statistical error. Uncertainty in the absolute rate constant scale estimated at about 50% (see text).

PAI rate constants. Figure 3 plots rate constants for process (1), as a function of probe intensity (with detuning less than 10 MHz) for polarization parallel and perpendicular to the atomic beam axis. The error bars reflect principally statistical uncertainties in the ion count rate. The principal source of systematic error lies in the determination of the interaction volume. Tight collimation of the atomic beam (0.3 cm diameter) centered within beam 3 (0.6 cm diameter) limits the transverse dimensions of the interaction volume. The length of the longitudinal dimension, along the atomic beam axis, is taken as the $1/e^2$ points of the Gaussian beam-3 profile. We estimate uncertainty in the interaction volume, due essentially to this longitudinal dimension, of 30%. Taking into account uncertainties in the ion detector efficiency and atomic beam density leads to an overall uncertainty in the absolute rate constant scale of Fig. 3 of 50%. It is worthwhile noting that the absolute magnitude of the PAI rate constants reported here at 5.3 mK are about an order of magnitude larger than those measured earlier in a MOT [13] with estimated temperature of 300 μK. Calculation of the absolute values and intensity dependence of the rate constants with a semiclassical OBE theory of the PAI process [14] also shows a marked increasing temperature dependence, but this theory, which does not include hyperfine structure, is too crude to correctly reflect intensity and polarization dependences. Meaningful interpretation of these effects will have to wait further development of the OBE theory. In summary we have used a single atomic beam to measure quantitatively the rate constant for an ultracold collision as a function of optical field intensity and polarization. The results show a marked intensity-dependent polarization effect.

R.N. acknowledges financial support from the Conselho Nacional de Desenvolvimento Científico e Tecnológico (CNPq). J.W. acknowledges support from the National Science Foundation and the National Institute of Standards and Technology. Acknowledgment is also made to the Donors of the Petroleum Research Fund, administered by the American Chemical Society, for partial support of this research.

[1] For accounts of early work on optical cooling, trapping, and ultracold collisions, see the special issues, J. Opt. Soc. Am. B **2**, 1706 (1985); **6**, 2020 (1989). Two more recent reviews are: P. S. Julienne, A. M. Smith, and K. Burnett, Adv. At. Mol. Opt. Phys. **30**, 141 (1993); T. Walker and P. Feng, *ibid.* **34**, 125 (1994).

[2] H. R. Thorsheim, J. Weiner, and P. S. Julienne, Phys. Rev. Lett. **58**, 2820 (1987).

[3] P. L. Gould, P. D. Lett, P. S. Julienne, W. D Phillips, H. R. Thorsheim, and J Weiner, Phys. Rev. Lett. **60**, 788 (1988).

[4] M. Wagshul, K. Helmerson, P. D. Lett, S. Rolston, W. D. Phillips, R. Heather, and P. S. Julienne, Phys. Rev. Lett. **70**, 2074 (1993); P. D. Lett, K. Helmerson, W. D. Phillips, L. P. Ratliff, S. L. Rolston, and M. E. Wagshul, *ibid.* **71**, 2200 (1993); J. D. Miller, R. A. Cline, and D. J. Heinzen, *ibid.* **71**, 2204 (1993).

[5] V. Bagnato, L. Marcassa, C. Tsao, Y. Wang, and J. Weiner, Phys. Rev. Lett. **70**, 3225 (1993).

[6] D. Hoffmann, P. Feng, R. S. Williamson, and T. Walker, Phys. Rev. Lett. **69**, 753 (1992), and references cited therein.

[7] C. D. Wallace, T. P. Dinneen, K.-Y. N. Tan, T. T. Grove, and P. L. Gould, Phys. Rev. Lett. **69**, 897 (1992).

[8] P. S. Julienne and R. Heather, Phys. Rev. Lett. **67**, 2135 (1991).

[9] P. Lett, P. Jessen, W. D. Phillips, S. Rolston, C. Westbrook, and P. Gould, Phys. Rev. Lett. **67**, 2139 (1991).

[10] H. R. Thorsheim, Y. Wang, and J. Weiner, Phys. Rev. A **41**, 2873 (1990).

[11] P. S. Julienne and F. H. Mies, J. Opt. Soc. Am. B **6**, 2257 (1989).

[12] P. M. Farrell, W. R. MacGillivray, and M. C. Standage, Phys. Rev. A **37**, 4240 (1983).

[13] V. Bagnato, L. Marcassa, Y. Wang, J. Weiner, P. S. Julienne, and Y. B. Band, Phys. Rev. A **48**, R2523 (1993).

[14] P. S. Julienne and Y. B. Band (unpublished).